Aspect Ratio-Dependent Twisting Motions in Photomechanical Molecular Crystal Ribbons via Solid-State [2 + 2] Photodimerization

Xiao-Dong Qiu,[a] Jun Lu,[a] Da-Hui Qu,[a] Fei Tong*[a]

a. Key Laboratory for Advanced Materials and Joint International Research Laboratory of Precision Chemistry and Molecular Engineering, Feringa Nobel Prize Scientist Joint Research Center, Frontiers Science Center for Materiobiology and Dynamic Chemistry Institute of Fine Chemicals, School of Chemistry and Molecular Engineering, East China University of Science and Technology 130 Meilong Road, Shanghai, 200237 (China)

E-mail of the Corresponding Author:

feitong@ecust.edu.cn,

Compound Synthesis

Synthesis of methyl (2*E*,4*E*)-2-cyano-5-phenylpenta-2,4-dienoate (**MCPD**): 1.32 g (0.01 mol) of cinnamaldehyde and 0.99 g (0.01 mol) of methyl cyanoacetate were added to 30 ml of toluene. To effectively catalyze the reaction, 0.2 ml of 4-methylpiperidine was slowly added. The reaction was refluxed with stirring at 110 °C for 4 hours to ensure complete conversion. After completion, the reaction mixture was naturally cooled to room temperature, and a yellow crystalline solid was observed upon placing in an ice bath at 0 °C. The product was isolated by filtration, and the filter cake was washed with an appropriate amount of methanol to remove trace impurities, yielding a yellow crystalline crude product. Recrystallization from dichloromethane (DCM) was performed as follows: The yellow crystalline crude product was dissolved in approximately 10 mL of DCM, and the mixture was heated at 60 °C with stirring for 10 minutes until complete dissolution. After cooling the solution to room temperature, approximately 30 mL of methanol was slowly added at 0 °C to induce full precipitation of the pure crystalline product. The yellow crystals of **MCPD** were synthesized under dark conditions. The target product was dried and stored in a brown bottle wrapped with aluminum foil to prevent light exposure.

When submitting the sample for nuclear magnetic resonance (NMR) analysis, the NMR tube was wrapped with aluminum foil to avoid light interference during measurement. (Figure S1). ^{1}H NMR (400 MHz, Acetone) δ 8.15, 8.12, 7.76, 7.67, 7.63, 7.48, 7.37, 7.34, 7.30, 3.86.(Figure S2). ^{13}C NMR (101 MHz, Acetone-d_6) δ 205.24, 162.40, 155.41, 149.44, 135.11, 131.08, 129.18, 128.59, 128.53, 122.79, 114.05, 104.02, 52.39, 29.52, 29.33, 29.14, 28.95, 28.75, 28.56, 28.37.(Figure S3). (HR-MS (ESI)): calculated for $C_{13}H_{11}NO_2$, [M] = 213.0790, found [M+1] = 214.0852 (Figure S4).

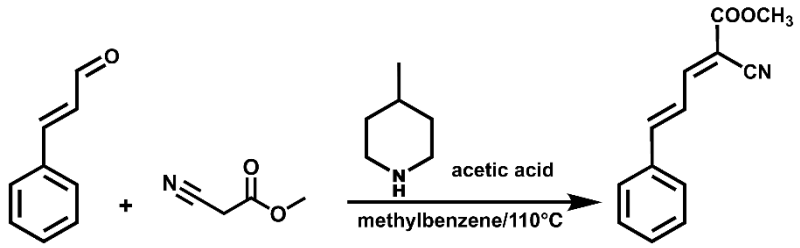

Fig. S1. Produces of synthesizing **MCPD** molecule.

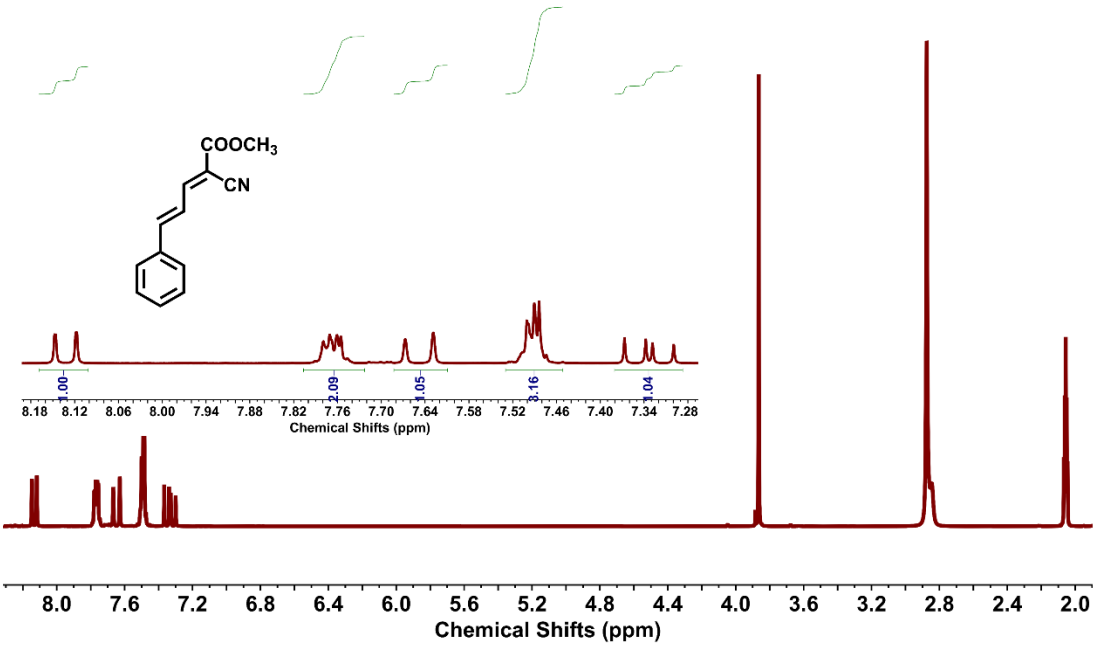

Fig. S2. ^{1}H NMR of **MCPD**. The peak near 2.05 ppm is from solvent, the peak near 2.87 is due to residue water. Inset: The enlarged region between 7.28 and 8.18 ppm (acetone-d_6 as solvent).

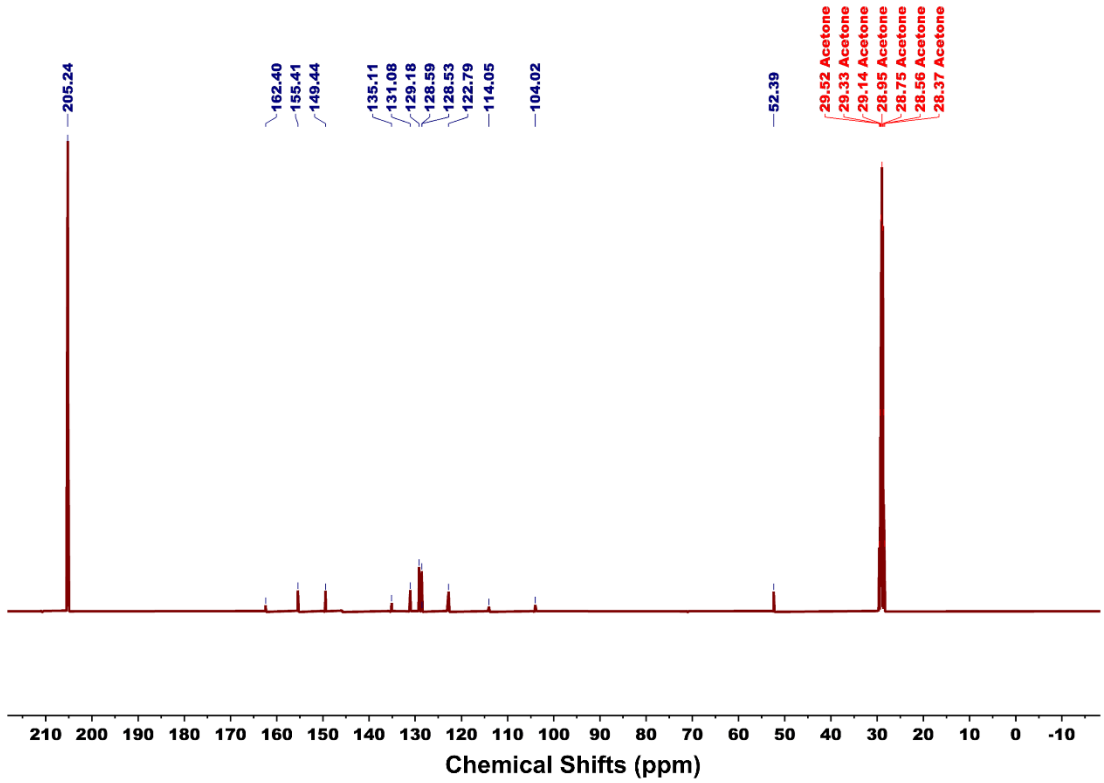

Fig. S3. ^{13}C NMR spectrum of **MCPD**. The peak around 29 ppm is due to solvent (acetone-d_6 as solvent).

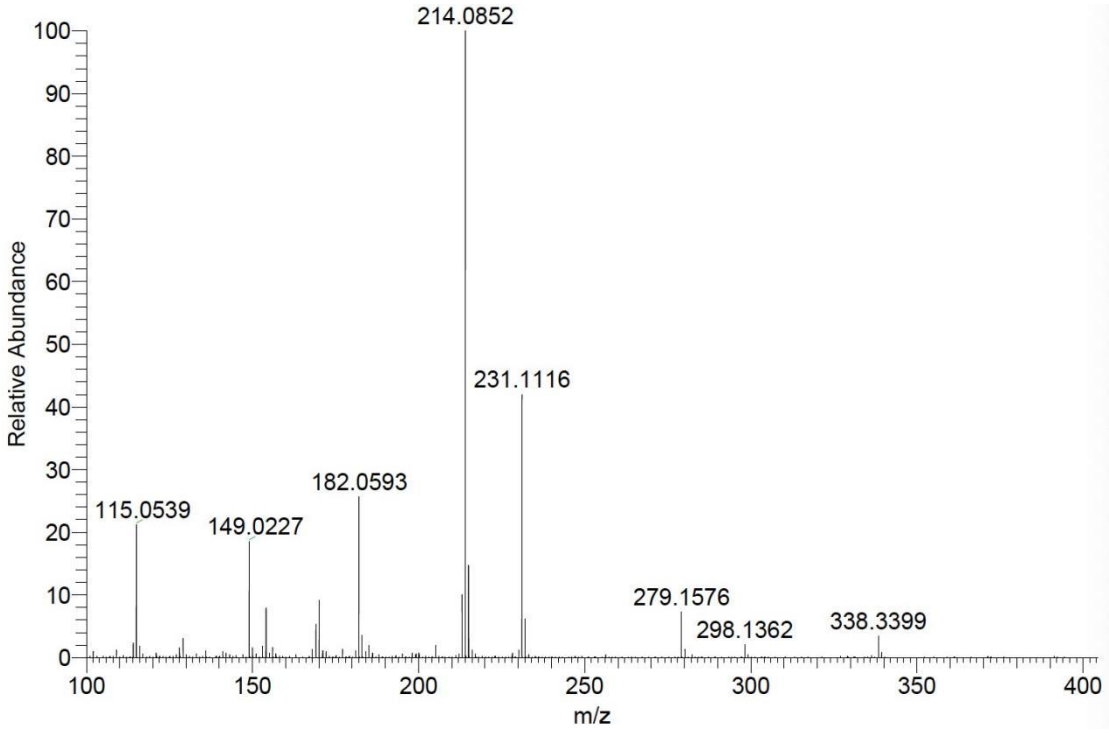

Fig. S4. HR-MS (ESI) spectrum of **MCPD**.

Single Crystal Structure Information

Table S1. Crystal data and structure refinement for **MCPD** monomer (CCDC:2520666)

Identification code	**MCPD** monomer	
Empirical formula	C_{13} H_{11} N O_2	
Formula weight	213.23	
Temperature	170.00 K	
Wavelength	1.34139 Å	
Crystal system	Triclinic	
Space group	P-1	
Unit cell dimensions	a = 7.1629(4) Å	α = 103.649(2)°.
	b = 7.8641(4) Å	β = 95.695(2)°.
	c = 11.2471(6) Å	γ = 113.196(2)°.
Volume	552.63(5) $Å^3$	
Z	2	
Density (calculated)	1.281 Mg/m^3	
Absorption coefficient	0.451 mm^{-1}	
F(000)	224.0	
Crystal size	0.17 x 0.17 x 0.05 mm^3	
Theta range for data collection	3.603 to 54.927°.	
Index ranges	-8<=h<=8, -8<=k<=9, -13<=l<=13	
Reflections collected	7711	
Independent reflections	2086 [R(int) = 0.0780]	
Completeness to theta = 53.594°	98.9 %	
Absorption correction	Semi-empirical from equivalents	
Max. and min. transmission	0.7508 and 0.5346	
Refinement method	Full-matrix least-squares on F^2	
Data / restraints / parameters	2086 / 0 / 146	
Goodness-of-fit on F^2	1.071	
Final R indices [I>2sigma(I)]	R1 = 0.0481, wR2 = 0.1301	
R indices (all data)	R1 = 0.0559, wR2 = 0.1374	
Largest diff. peak and hole	0.245 and -0.274 $e.Å^{-3}$	

Table S2. Crystal data and structure refinement for *d*-**MCPD** (CCDC:2520711).

Identification code	**MCPD** photodimer	
Empirical formula	$C_{26}H_{22}N_2O_4$	
Formula weight	426.45	
Temperature	298 K	
Wavelength	1.54178 Å	
Crystal system	Triclinic	
Space group	P-1	
Unit cell dimensions	a = 7.4552 (8) Å	α = 72.773(6)°.
	b = 7.6250(6) Å	β = 89.286(8)°.
	c = 11.4156(8) Å	γ = 70.571(7)°.
Volume	581.85(9) $Å^3$	
Z	1	
Density (calculated)	1.217 Mg/m^3	
Absorption coefficient	0.673 mm^{-1}	
F(000)	224.0	
Crystal size	0.05 x 0.03 x 0.03 mm^3	
Theta range for data collection	4.1° to 68.2°.	
Index ranges	-8<=h<=8, -8<=k<=9, -13<=l<=13	
Reflections collected	8081	
Independent reflections	2128 [R(int) = 0.075]	
Completeness to theta = 53.594°	99.9 %	
Absorption correction	multi-scan SADABS2016/2 (Bruker, 2016/2)	
Max. and min. transmission	0.754 and 0.671	
Refinement method	Full-matrix least-squares on F^2	
Data / restraints / parameters	2128 / 0 / 146	
Goodness-of-fit on F^2	1.017	
Final R indices [I>2sigma(I)]	R1 = 0.0886, wR2 = 0.1876	
R indices (all data)	R1 = 0.0943, wR2 = 0.2946	
Largest diff. peak and hole	0.57 and -0.39 $e.Å^{-3}$	

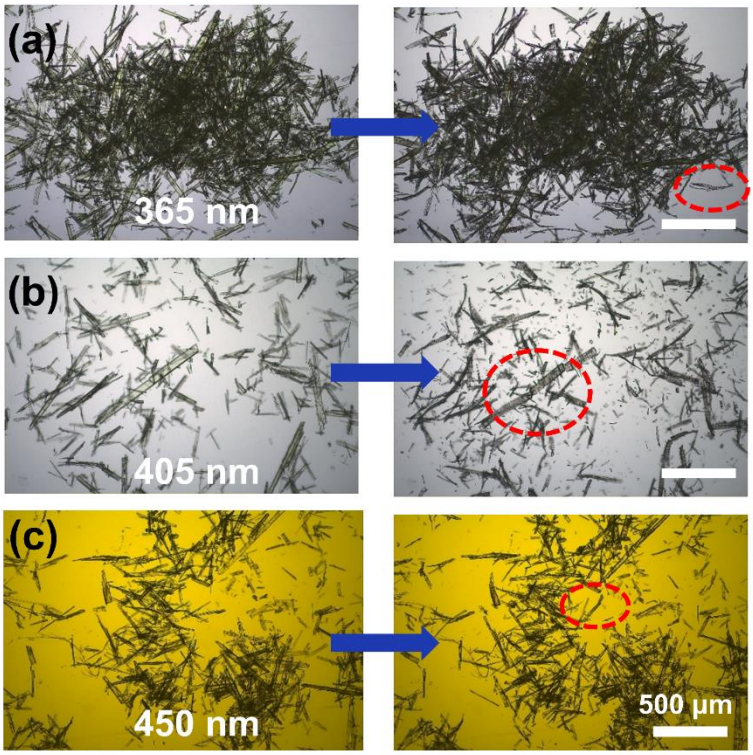

Fig. S5. Optical microscope images of **MCPD** powder before and after exposure to (a) 365 nm, (b) 405 nm, and (c) 450 nm light, revealing that the powder undergoes fragmentation, splitting, and jumping behaviors upon illumination.

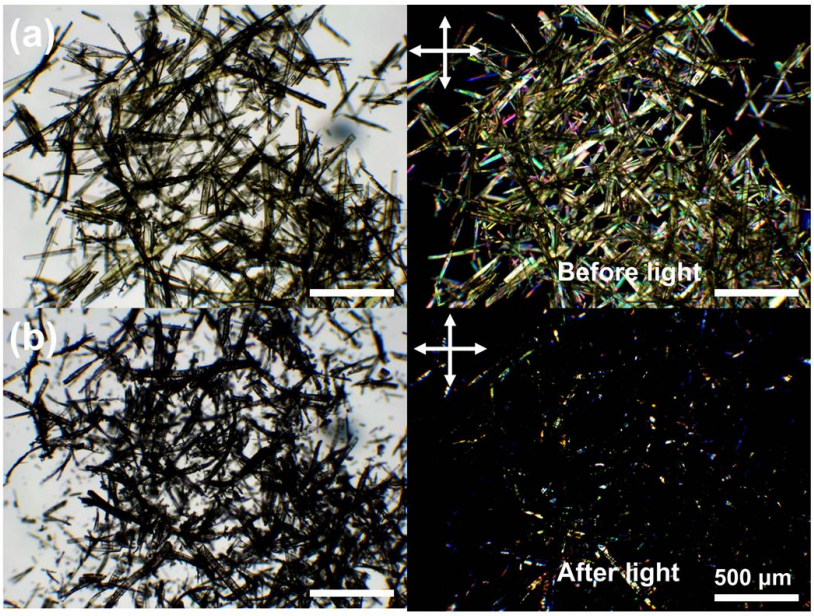

Fig. S6. (a) Optical and cross-polarized microscopy images of **MCPD** powder before light irradiation. (b) Images after irradiation, showing fragmentation of the solid powder while partial crystallinity is retained.

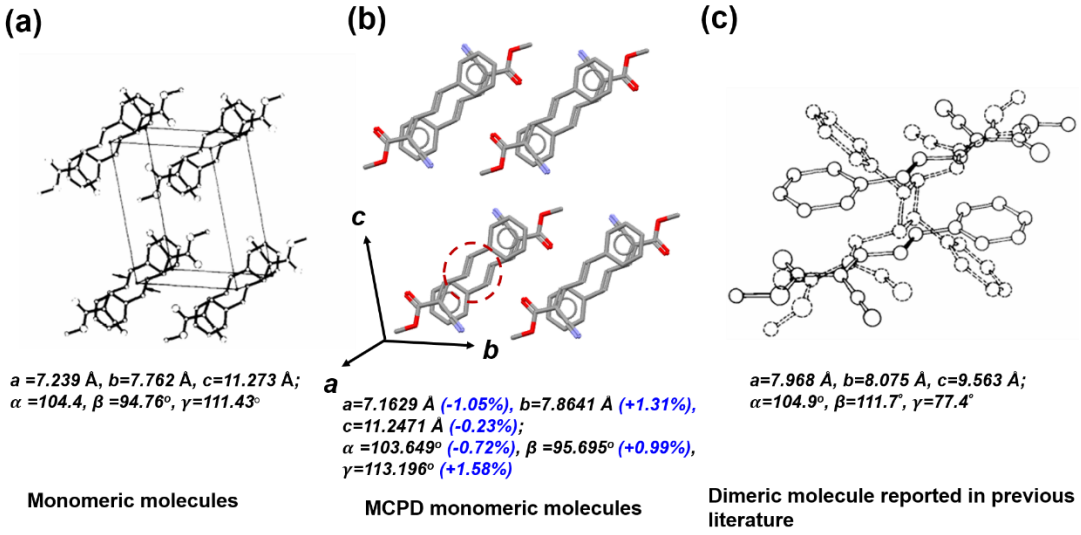

Fig. S7. (a) Monomeric molecular packing structure reported in previous literature. (b) **MCPD** monomeric molecular packing structure viewed from the same direction, showing identical packing and almost identical crystallographic parameters. The red-dashed circle indicates the structure can undergo photodimerization, similar to the arrows in (a). (c) The dimeric molecular packing structure reported in the literature was obtained via solvent-based crystal growth.

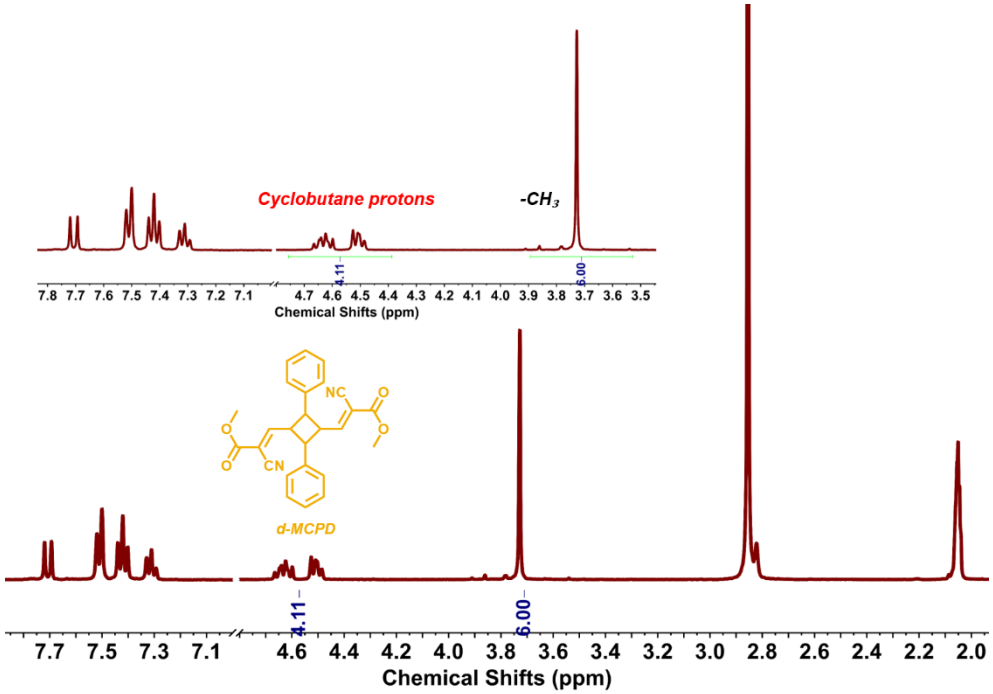

Fig. S8. ^{1}H NMR spectrum of the *d*-**MCPD** with the magnified region showing the cyclobutane proton formation.

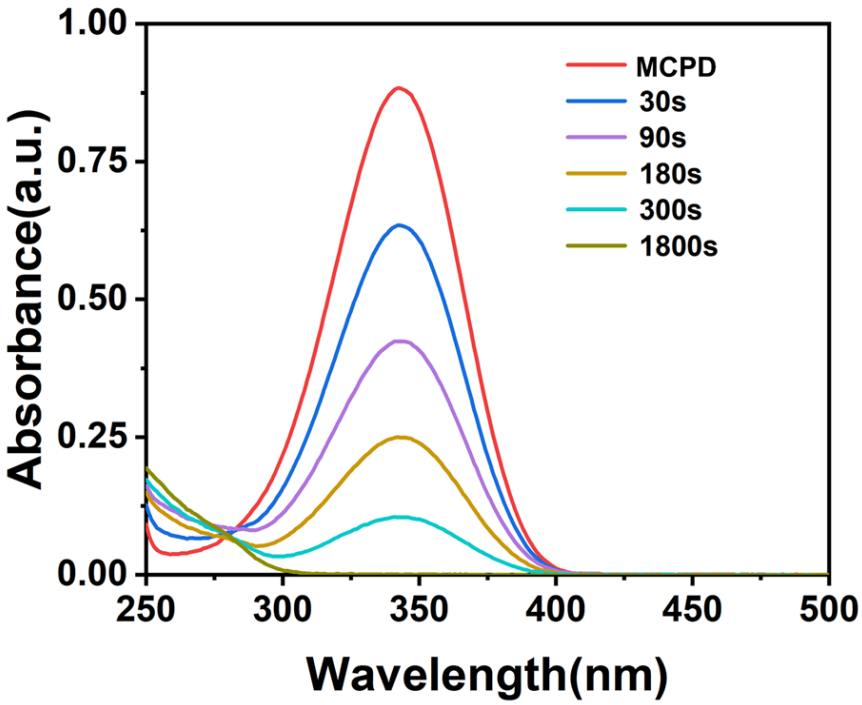

Fig. S9. UV-vis absorption spectra of the photo-reacted **MCPD** solids dissolved in THF after different durations of light irradiation.

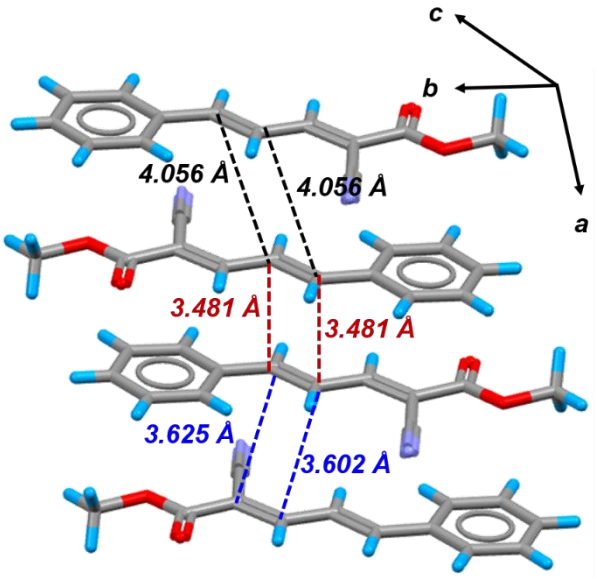

Fig. S10. The molecular packing structure of **MCPD** in the crystal lattice, showing the different intermolecular distances at the C=C bonds between two head-to-tail oriented molecules. These distances, including 3.481Å, 3.602 Å, 3.625 Å, and 4.056 Å, allow for [2 + 2] photodimerization according to the Schmidt topochemistry principle.

Fig. S11. Schematic illustration of the preparation of **MCPD** crystalline ribbons.

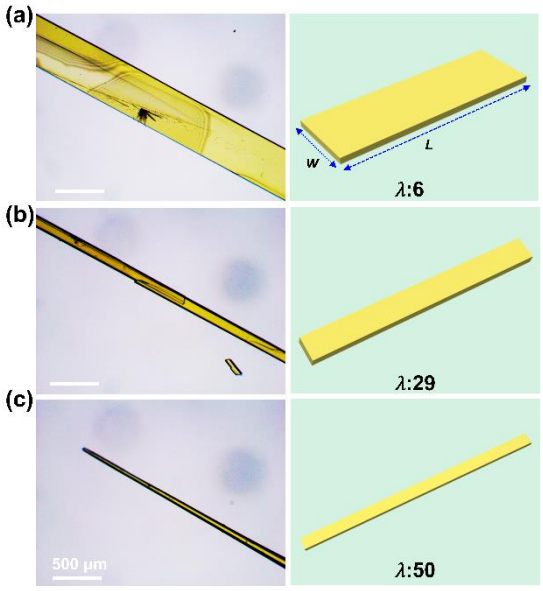

Fig. S12. Optical microscope images of **MCPD** crystals with varying aspect ratios, accompanied by corresponding schematic illustrations of their crystal structures.

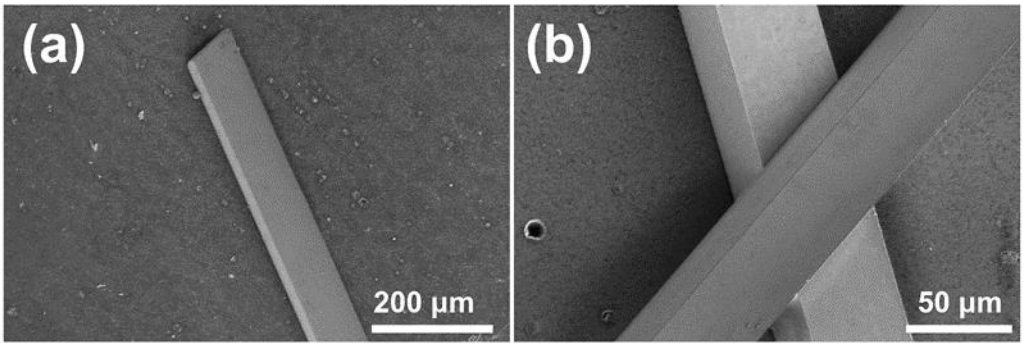

Fig. S13. SEM images of **MCPD** single crystal ribbons, revealing a regular and well-defined surface.

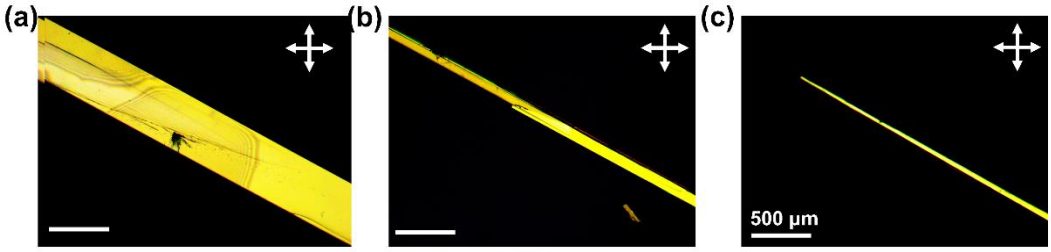

Fig. S14. Cross-polarized microscope images of **MCPD** crystals before light irradiation, revealing high crystallinity.

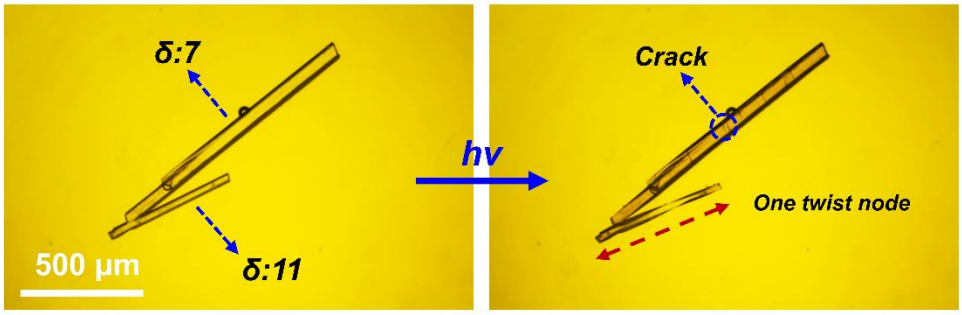

Fig. S15. When the δ value is between 8 and 25, the more slender **MCPD** ribbons twist rather than crack, producing a single twist node upon light irradiation

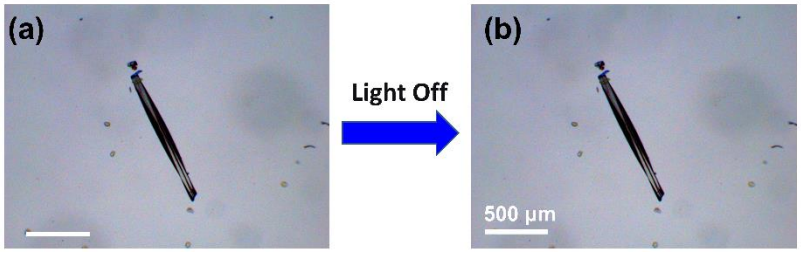

Fig. S16. These branched sub-ribbons also exhibit single-pitch twisting upon light irradiation. The twisted morphology was maintained after the excitation light was switched off

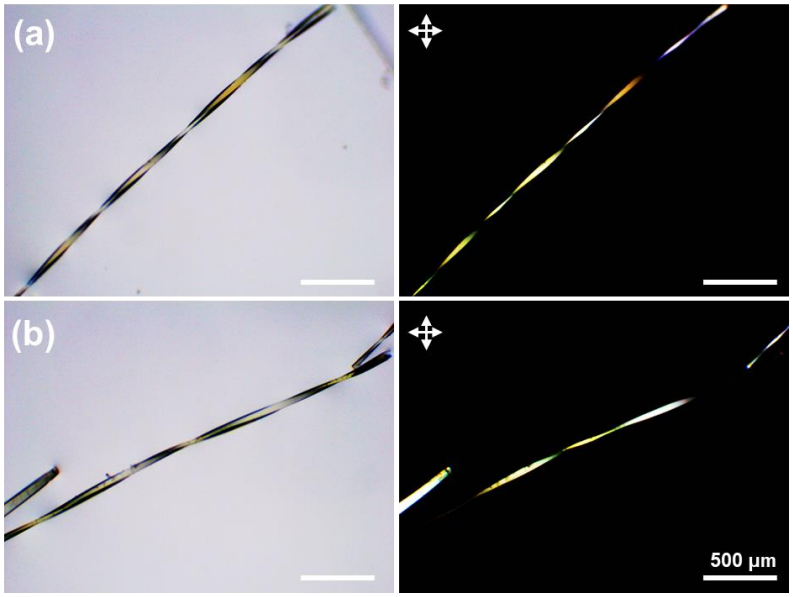

Fig. S17. Upon turning off the light, both the twisted morphology and crystallinity remain unchanged.

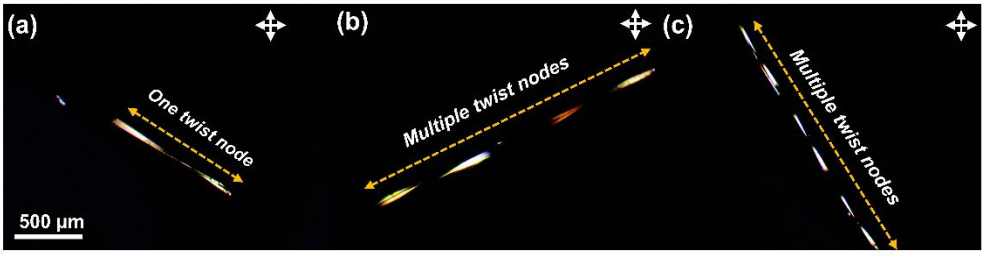

Fig. S18. Besides retaining the spirally twisted morphology, these light-irradiated ribbons still exhibit birefringence under a cross-polarized microscope, indicating a crystal-to-crystal transformation.

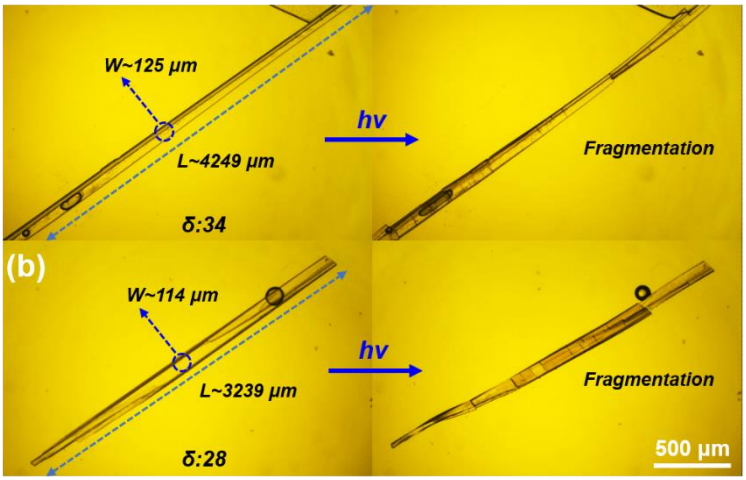

Fig. S19. Optical microscope images of **MCPD** ribbons with high δ values showing cracking and fragmentation after light irradiation.

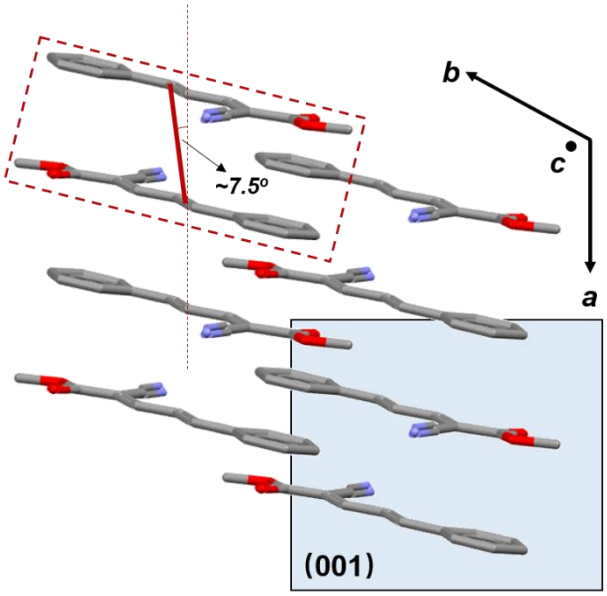

Fig. S20. Molecular orientation in the **MCPD** crystal lattice shows that the photodimerization direction aligns approximately 7.5° with the crystallographic *a*-axis.

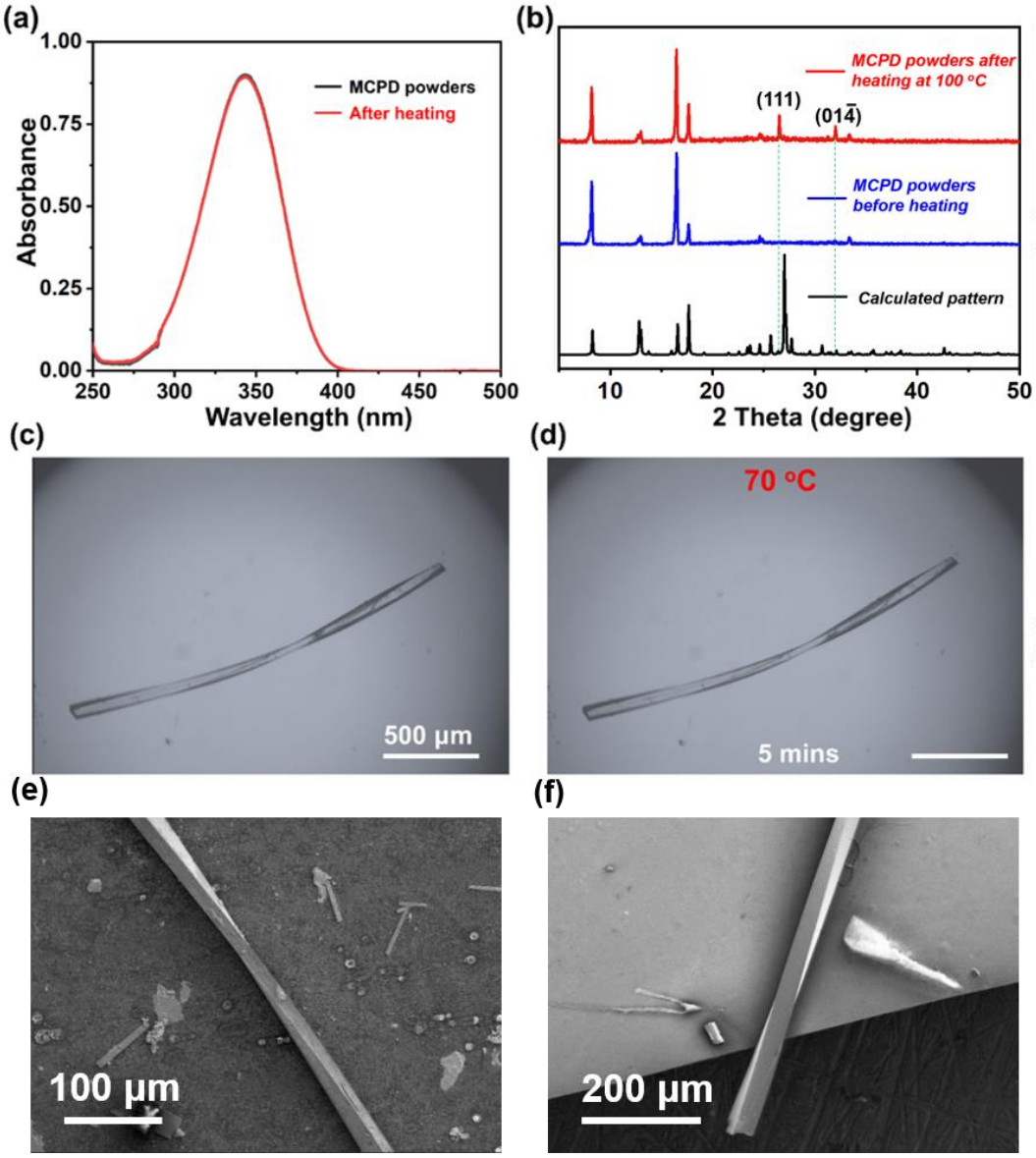

Fig. S21. (a) Comparative UV-Vis absorption spectra of **MCPD** powder dissolved in THF before and after heating. (b) Comparative PXRD patterns of **MCPD** powder before (dark blue) and after heating (red) with the calculated pattern based on single crystal structures (black). (d) Helical crystals of **MCPD** after heating at 70°C for 5 minutes, showing no significant morphological change. (e-f) SEM images of **MCPD** helical crystals, revealing regular and smooth surfaces.

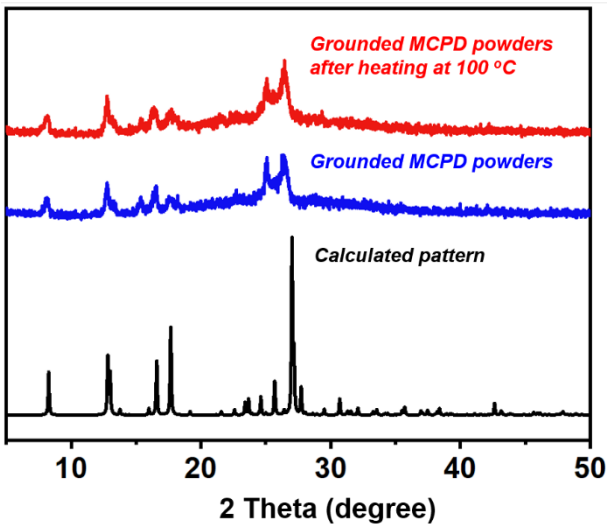

Fig. S22. Comparative PXRD analysis of milled **MCPD** powders before (dark blue) and after heating with the calculated pattern based on single crystal structures (black).

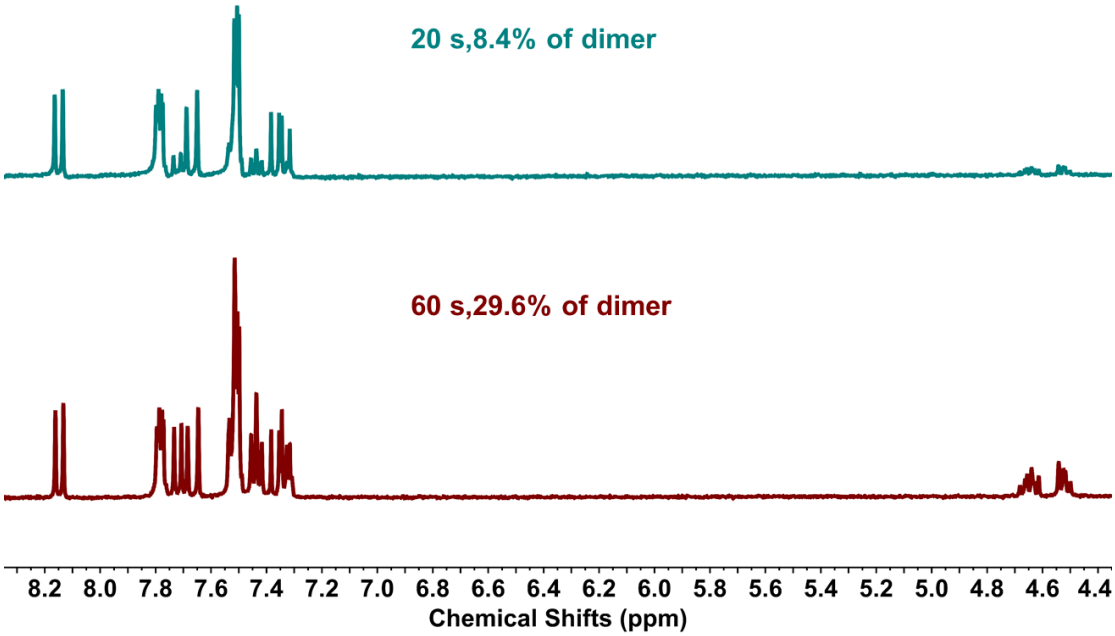

Fig. S23. ^{1}H NMR spectrum of the **MCPD** ribbon upon cessation of twisting, revealing approximately 30% *d*-**MCPD**.

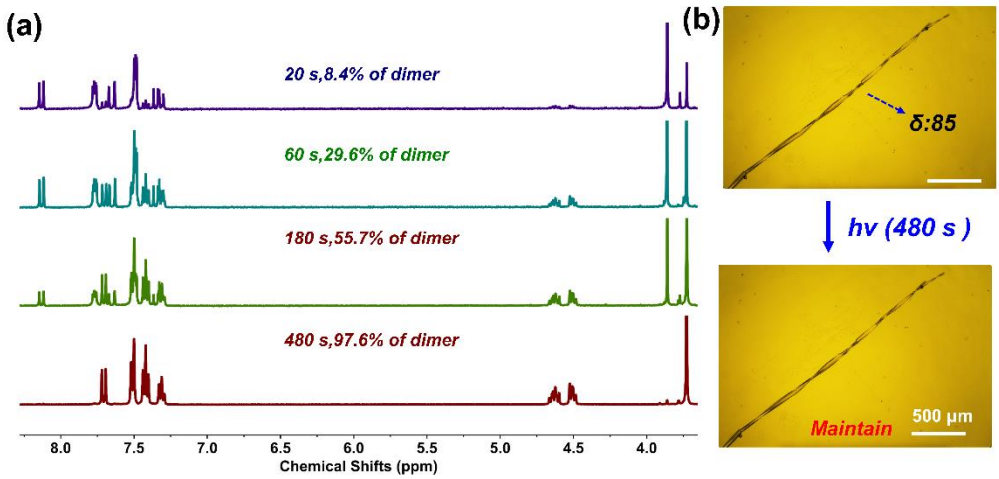

Fig. S24. (a) Prolonged light irradiation increases the *d*-**MCPD** content in the twisted crystal. (b)While prolonged light irradiation does not enhance the twisted morphology.

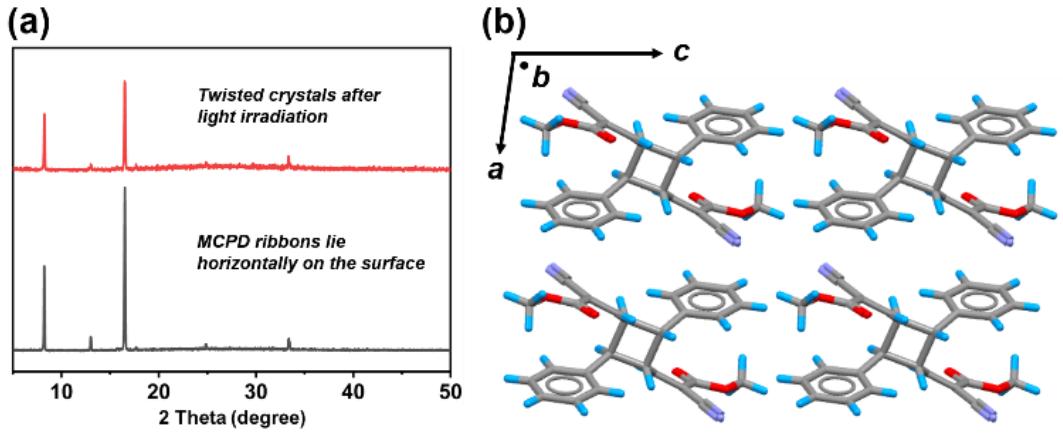

Fig. S25. (a) PXRD patterns of twisted crystals after light irradiation and **MCPD** ribbons before light irradiation. (b) Molecular orientation in the *d*-**MCPD** crystal lattice viewed along the crystallographic *b*-axis.

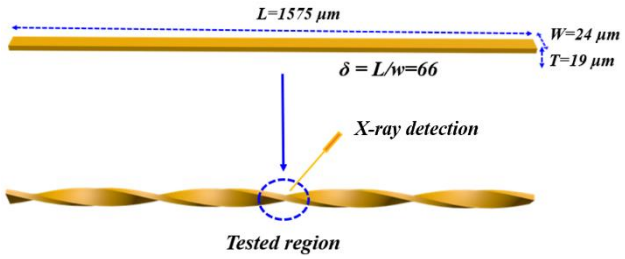

Fig. S26. A schematic diagram illustrating the preparation of *d*-**MCPD** single crystals. The water-surface-floating-droplet method yielded single-crystal **MCPD** rods. Subsequent selection of a crystal with approximate dimensions of 1575 μm × 24 μm × 19 μm enabled irradiation with 450 nm light (Intensity ~20 mW/cm^2, Irradiation duration: 3-5 minutes). This photoirradiation drove near-quantitative conversion to the corresponding photodimer. Final analysis proceeded following excision of a segment near the twisted region using a sampling needle.

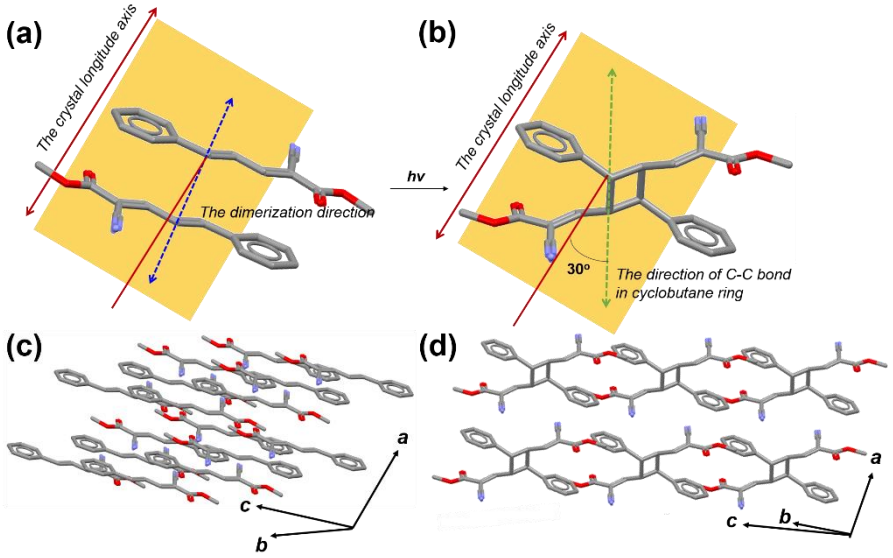

Fig. S27 (a) A pair of **MCPD** monomeric molecules in the crystal lattice shows that the dimerization direction has a small angle (~7.5°) with the crystal ribbon longitude axis. (b) The formed *d*-**MCPD** molecule is viewed along the same direction in the crystal lattice, showing an approximately 30° angle between the C-C bond in the cyclobutane ring and the crystal ribbon's longitudinal axis after photodimerization, inducing internal strain in the lattice. (c)-(d) Molecular packing structures of **MCPD** and *d*-**MCPD** viewed along the same direction.

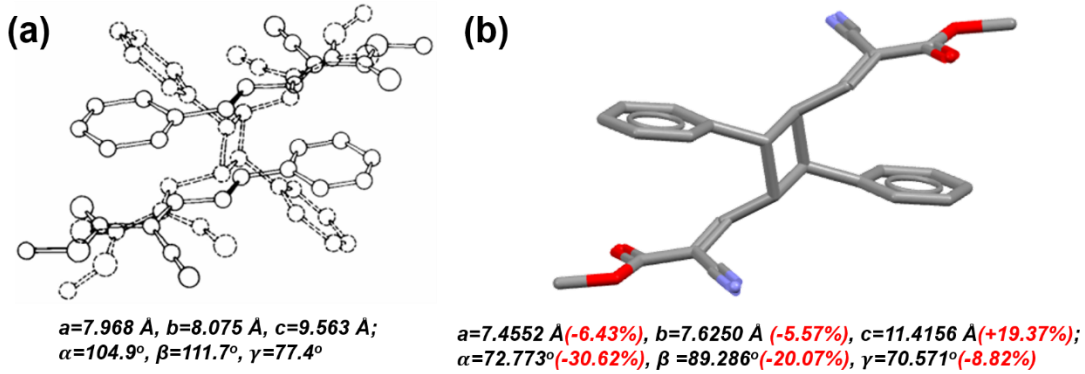

Fig. S28. (a) The dimeric structure in the crystal lattice that was obtained through recrystallization. (b) The molecular structure of *d*-**MCPD** in the crystal lattice that was determined by measuring a fully photo-reacted twisted ribbon.

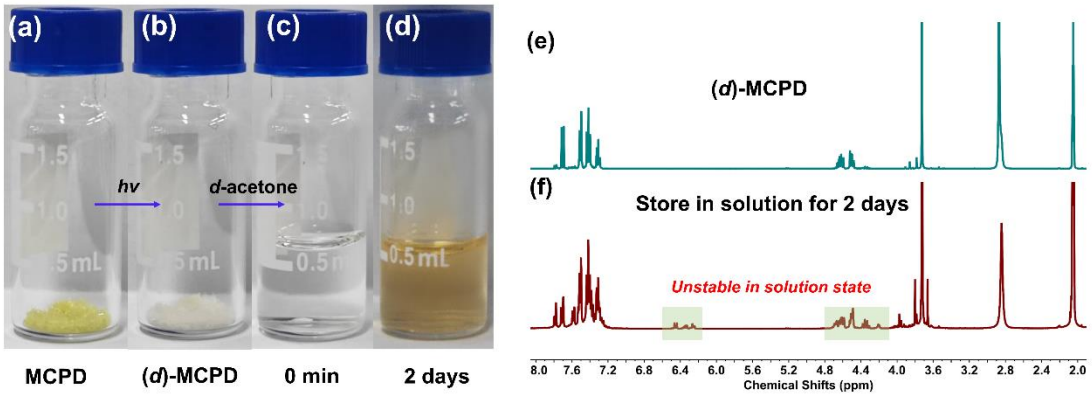

Fig. S29. Snapshots of **MCPD** solid powder in a glass vial: (a) before and (b) after 60-minute irradiation with 405 nm light (intensity ~120 mW/cm²); (c) the sample after photoreaction dissolved in acetone-d_6; (d) the solution from (c) after being stored in the dark at room temperature for 2 days. (e) ^{1}H NMR spectrum of *d*-**MCPD**. (f) ^{1}H NMR spectrum of *d*-**MCPD** after two days of storage in the dark. The spectral changes observed in (f) indicate that *d*-**MCPD** is unstable in solution.